

**The
Vibratory Stress Relief
Library**

REPRINT:

**EVALUATING THE EFFECTIVENESS
OF VIBRATORY STRESS RELIEF BY A
MODIFIED HOLE-DRILLING METHOD**

**G.-C. Luh
R.-M. Hwang**

**Published in The International Journal
Of Advanced Manufacturing Technology**

1998

Evaluating the Effectiveness of Vibratory Stress Relief by a Modified Hole-Drilling Method

G.-C. Luh and R.-M. Hwang

Department of Mechanical Engineering, Tatung Institute of Technology, Taipei, Taiwan

In this paper, a modified through hole-drilling method is developed to evaluate the effectiveness of the application of vibratory stress relief (VSR). The principal residual stresses at any specified point before and after the treatment of VSR are measured by this method with the same cemented commercially available three-element strain gauge rosette. By comparing the magnitude of the measured results, the effectiveness of the treatment of VSR can thus be determined. Thin butt-welded specimens are prepared to verify the accuracy of the modified hole-drilling method compared to that of the conventional hole-drilling method. The experimental results show that the percentages of the relative errors between these two methods are all within 2.9%. Therefore, this modified method shows good accuracy in the determination of residual stresses before and after VSR. Meanwhile, the maximum principal residual stresses at the measured points are effectively reduced by about 5.8% to 27% after the application of VSR, and the minimum principal residual stresses at the measured points are effectively reduced by about 9.6% to 31%.

Keywords: Hole-drilling method; Residual stress; Resonant frequency; Strain gauge rosette; TIG welding process; Vibratory stress relief (VSR)

1. Introduction

Residual stresses are inevitably generated in manufactured machine elements, especially in the welding region of the weldment because of its relatively high residual stresses values. The existence of the residual stresses in the machine elements may cause undesirable premature fracture, stress corrosion cracking, and dimensional instability. Distortion usually occurs owing to the relaxation of the residual stresses during storage, transportation, machining, assembly, or operation. Thus the

reduction or elimination of the locked-in residual stresses is an essential procedure during the manufacturing processes.

The common methods generally adopted for this purpose include natural ageing, shot peening [1], ultrasonic treatment [2], thermal stress relief (TSR) [3,4], vibratory stress relief (VSR) [5-17], etc. TSR is the most widely used and effectively proven technology. Its influencing parameters, including soaking temperature, time duration, heating rate, and cooling rate, can be examined and operated according to the specifications shown in the ASM handbook. However, the treatment of TSR has several drawbacks. The cost of both the equipment and the energy involved is high, the process is time consuming, an oxide scale may be induced on the surface, and some of the mechanical properties such as hardness, strength, and stiffness may be adversely affected owing to metallurgical changes.

The treatment of VSR has been demonstrated to possess some degree of effectiveness for stress relief [6-17], to lower the peak residual stresses significantly, and to smooth the distribution of the residual stresses in the weldment [6]. So, the application of VSR is a practical alternative to TSR for the reduction of the residual stresses in machine elements and structures, and does not bring about the same problems as mentioned above. As the physical explanation of the mechanism for relieving the residual stresses is incomplete, and the quantitative data for verifying the effectiveness of stress relief is insufficient, the application of VSR has been restricted until now.

August and Hebel [7] have demonstrated that the treatment by VSR at subresonant frequency can efficiently relieve the residual stresses in low and medium carbon steel, stainless steel, aluminium alloys, etc. However, some investigators [8-15] proposed that the existing residual stresses can be effectively reduced only when the machine elements are excited at one or more resonant frequencies, and gave experimental results to show the extent of the effect after the treatment of VSR. In these investigations, the methods used to evaluate the effectiveness of the treatment of VSR can be classified as follows:

1. *Magnitude of the distortion after VSR or machining:* The residual stresses are estimated by the magnitude of the distortion after VSR [5], or the maintenance of the dimensional stability of the vibratory stress-relieved machine elements dur-

Correspondence and offprint requests to: Dr G.-C. Luh, Department of Mechanical Engineering, Tatung Institute of Technology, 40 Chungshan N Road, 3rd Sec, Taipei 10451, Taiwan. E-mail: gluh@mgher.tit.edu.tw

ing the subsequent machining processes [17]. Because the distortion measured under the aforementioned condition is quite limited, the locked-in residual stresses cannot be determined accurately. Thus, it would be better to verify the effectiveness of the VSR with other methods before the machine element is machined.

2. *Destructive methods:* The methods used include layer removal by sawing or single-point fly-cutting [8,15], the Sachs boring-out technique [6], the technique devised by Rosenthal and Norton [9], etc. Since the machine elements will be destroyed by these methods, and some extraneous residual stresses will be introduced into the machine elements, these methods are not suitable for realistic engineering application.

3. *Decrease of the resonant frequency:* The resonant frequency of the machine element has been shown to decrease slightly as the existing residual stresses are reduced after treatment by VSR [7,10]. However, the decrease of the resonant frequency is not influenced by the reduction of the residual stresses alone [15]. Therefore, the approach mentioned above is not a precise method for verifying the effectiveness of VSR.

4. *X-ray diffraction method* [11,16]: Because it is not possible to guarantee that the measured point before VSR remains the same after VSR, and the experimental equipment is relatively expensive, this method is not suitable for practical application.

5. *Conventional hole-drilling method:* Two strain gauge rosettes are cemented separately at correspondingly symmetric positions where the original stresses are assumed to be identical, with one of the rosettes used to measure the residual stresses before VSR and the other used to measure the residual stresses after VSR [17]. The effectiveness of the VSR treatment is determined by the residual stresses measured by these two rosettes. Since there may be no geometrically symmetrical positions in a real manufactured structure, particularly for the sophisticated ones, and the original residual stresses locked in these two measured points, even though their geometries are near symmetric, may not be exactly identical, the application of the conventional hole-drilling method in this condition is restricted.

In order to avoid the problems in the conventional hole-drilling method, a modified through hole-drilling method suitable for realistic engineering applications is described in this paper to determine the effectiveness of the VSR treatment. The residual stresses at the same defined point before and after the VSR treatment can be measured by this modified method, and the effectiveness of the application of VSR can consequently be determined.

2. Theoretical Analysis

2.1 A Brief Discussion of the Modified Hole-Drilling Method

The purpose of this investigation is to develop a through hole-drilling method to determine the effectiveness of treatment by

VSR. The residual stresses before and after VSR are measured by this method with the commercially available three-element strain gauge rosette that is cemented at any specified point. By comparing the values of the measured results, the effectiveness of the VSR treatment can be determined. Figure 1 displays the radial stress distribution before and after hole drilling in a thin plate under a uniform uniaxial residual stress field as shown in Fig. 2.

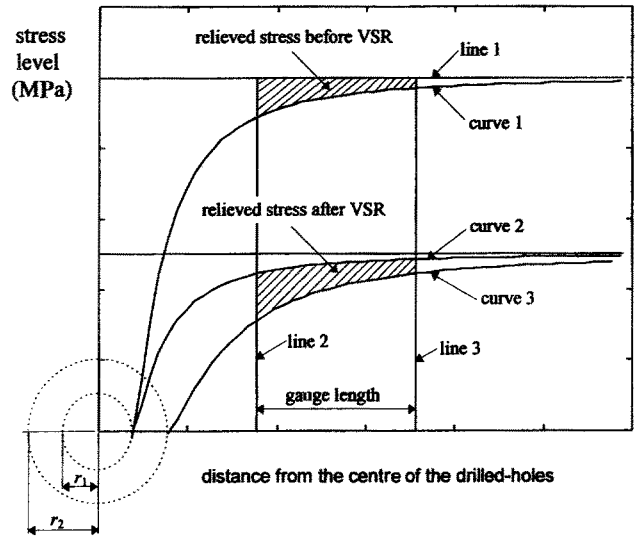


Fig. 1. Schematic diagram of the amount of the relieved stresses before and after VSR treatment.

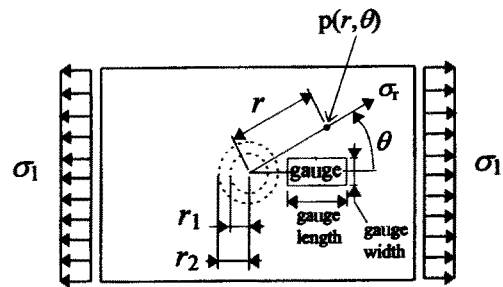


Fig. 2. Diagram of a strain gauge cemented (in the direction of $\theta = 0^\circ$) on a thin plate that is subjected to a uniform uniaxial stress field.

Before the treatment of VSR, line 1 and curve 1 represent, respectively, the distribution of the stress before and after drilling a small hole with a radius r_1 . Lines 2 and 3 indicate the edges of the strain gauge in the radial direction. The hatched area surrounded by lines 1–3 and curve 1 is the relieved stress after drilling a small hole with a radius r_1 before VSR.

After the VSR treatment, curve 2 denotes the distribution of the stress after drilling a small hole with a radius r_1 , and curve 3 represents the distribution of the stress after enlarging the small hole with a radius r_2 . Then the hatched area surrounded by lines 2 and 3 and curves 2 and 3 is the relieved stress after enlarging the small hole after VSR.

Since the difference between the radii of the two concentric drilled holes is quite small, the measured principal residual stresses before and after enlarging the minor hole, as discussed

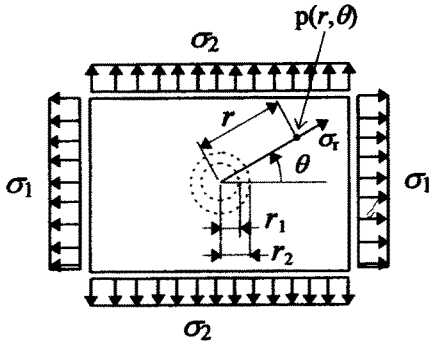


Fig. 3. A thin plate subjected to a uniform biaxial stresses field.

above, can be assumed to be the principal residual stresses before and after VSR at the same measured point. Hence, after the magnitude of the residual stresses before and after the VSR treatment is acquired, the effectiveness of VSR can be evaluated. The theory of this method will be discussed in the following sections.

2.2 Measurement of the Residual Stresses Before VSR

Schajer [18] has shown that the measured relieved strains depend upon only the residual stresses originally locked at the boundary of the drilled hole. The residual stresses beyond the boundary of the drilled hole would not affect the measured relieved strains. Therefore, the residual stresses determined by the hole-drilling method are localised values, initially existing at the boundary of the small drilled hole.

Figure 3 shows the condition of a thin plate subjected to uniform biaxial residual stresses. Before the VSR treatment, the radial relieved strain [19–21], after the drilling of a minor hole with a radius of r_1 at any point $p(r, \theta)$, can be expressed as

$$\epsilon_{rb} = \sigma_1(A + B\cos 2\theta) + \sigma_2(A - B\cos 2\theta) \quad (1)$$

where

$$A = -[(1+\nu)/(2E)](r_1^2/r^2)$$

$$B = -[(1+\nu)/(2E)]\{[4/(1+\nu)](r_1^2/r^2) - 3r_1^4/r^4\}$$

Since any strain gauge possesses a finite area rather than being an infinitesimal point, the effect of the gauge area on the

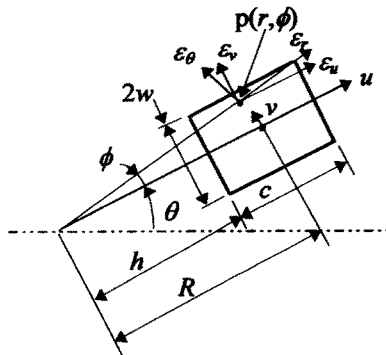


Fig. 4. Schematic representation of a strain gauge.

relieved strain should be taken into consideration. Figure 4 shows a schematic representation of a strain gauge with a finite area instead of a point $p(r, \theta)$ displayed in Fig. 3. During the experimental process, the sensitivity of the transverse relieved strain designed in the commonly used strain gauge rosette is ignored as its value is quite small compared to the sensitivity of the longitudinal relieved strain. So, only the longitudinal relieved strain is required in the measurement of the residual stress. The longitudinal relieved strain for a strain gauge at any point $p(r, \phi)$ can be expressed as [22]:

$$\epsilon_{ub} = \{- (1+\nu)[r_1^2/(2r^2)](\sigma_1 + \sigma_2)\cos 2\phi - (1 - \nu)(r_1^2/r^2)(\sigma_1 - \sigma_2)\cos 2(\theta + \phi) + [(1+\nu)/2](-2r_1^2/r^2 + 3r_1^4/r^4)(\sigma_1 - \sigma_2)\cos 2(\theta + 2\phi)\}/E \quad (2)$$

Moreover, the average longitudinal relieved strain of the strain gauge under its area can be obtained by the double integration [22,23] as follows:

$$\epsilon_{ub} = (1/2cw) \int_h^{h+c} \int_{-w}^w \epsilon_{ub} du dv \quad (3)$$

After integrating Eq. (3), the result can be expressed as:

$$\epsilon_{ub} = \mathbf{A}(\sigma_1 + \sigma_2)/E + [\mathbf{B}(\sigma_1 - \sigma_2)\cos 2\theta]/E \quad (4)$$

where

$$\mathbf{A} = [-(1+\nu)r_1^2/(2cw)]\{\tan^{-1}[(h+c)/w] - \tan^{-1}(h/w)\}$$

$$\mathbf{B} = [1/(2cw)]\{-2(1-\nu)r_1^2[\tan^{-1}((h+c)/w) - \tan^{-1}(h/w)] + (1+\nu)[-2r_1^2(-w(h+c)/((h+c)^2 + w^2) + wh/(h^2 + w^2)] + r_1^4(-w(h+c)/((h+c)^2 + w^2)^2 + wh/(h^2 + w^2)^2)\}$$

The three longitudinal relieved strains can be obtained after drilling a small hole with a radius r_1 through the centre of a commercially available three-element strain gauge rosette, as shown in Fig. 5; that is,

$$\epsilon_{ub}^1 = \mathbf{A}(\sigma_1 + \sigma_2)/E + [\mathbf{B}(\sigma_1 - \sigma_2)\cos 2\theta]/E \quad (5a)$$

$$\epsilon_{ub}^2 = \mathbf{A}(\sigma_1 + \sigma_2)/E + [\mathbf{B}(\sigma_1 - \sigma_2)\cos 2(\theta + 225^\circ)]/E \quad (5b)$$

$$\epsilon_{ub}^3 = \mathbf{A}(\sigma_1 + \sigma_2)/E + [\mathbf{B}(\sigma_1 - \sigma_2)\cos 2(\theta + 90^\circ)]/E \quad (5c)$$

Then the principal residual stresses and their directions before the VSR treatment can be calculated with the above three longitudinal relieved strains.

2.3 Measurement of the Residual Stresses after VSR

After the VSR treatment, the original biaxial residual stresses (σ_1 and σ_2) are assumed to be reduced to σ'_1 and σ'_2 . The distribution of the stresses in the vicinity of the hole (radius = r_1) at any point $p(r, \theta)$ can be expressed as follows:

$$\sigma'_r = (\sigma'_1 + \sigma'_2)(1 - r_1^2/r^2)/2 + (\sigma'_1 - \sigma'_2)(1 + 3r_1^4/r^4 - 4r_1^2/r^2)(\cos 2\theta)/2 \quad (6a)$$

$$\sigma'_\theta = (\sigma'_1 + \sigma'_2)(1 + r_1^2/r^2)/2 - (\sigma'_1 - \sigma'_2) \quad (6b)$$

$$\begin{aligned} & (1+3r_1^4/r^4)(\cos 2\theta)/2 \\ \tau_{r,\theta}' = & -(\sigma_1' - \sigma_2')(1-3r_1^4/r^4+2r_1^2/r^2)(\sin 2\theta)/2 \end{aligned} \quad (6c)$$

In order to obtain the magnitude of the residual stresses, the small hole is enlarged to a radius of r_2 . Then the distribution of the stresses in the vicinity of the hole (radius = r_2) yields the following expressions:

$$\sigma_r'' = (\sigma_1' + \sigma_2')(1-r_2^2/r^2)/2 + (\sigma_1' - \sigma_2') \frac{(1+3r_2^4/r^4 - 4r_2^2/r^2)(\cos 2\theta)/2}{(1+3r_1^4/r^4 - 4r_1^2/r^2)(\cos 2\theta)/2} \quad (7a)$$

$$\sigma_\theta'' = (\sigma_1' + \sigma_2')(1+r_2^2/r^2)/2 - (\sigma_1' - \sigma_2') \frac{(1+3r_2^4/r^4)(\cos 2\theta)/2}{(1+3r_1^4/r^4)(\cos 2\theta)/2} \quad (7b)$$

$$\tau_{r,\theta}'' = -(\sigma_1' - \sigma_2')(1-3r_2^4/r^4+2r_2^2/r^2)(\sin 2\theta)/2 \quad (7c)$$

So the measurement of the relieved stresses after enlarging the drilled hole can be acquired by subtracting Eq. (7) from Eq. (6):

$$\Delta\sigma_r = (\sigma_1' + \sigma_2')[(r_1^2 - r_2^2)/r^2]/2 + (\sigma_1' - \sigma_2') \frac{[4(r_1^2 - r_2^2)/r^2 - 3(r_1^4 - r_2^4)/r^4](\cos 2\theta)/2}{[4(r_1^2 - r_2^2)/r^2 - 3(r_1^4 - r_2^4)/r^4](\cos 2\theta)/2} \quad (8a)$$

$$\Delta\sigma_\theta = (\sigma_1' + \sigma_2')[-(r_1^2 - r_2^2)/r^2]/2 + (\sigma_1' - \sigma_2') \frac{[3(r_1^4 - r_2^4)/r^4](\cos 2\theta)/2}{[3(r_1^4 - r_2^4)/r^4](\cos 2\theta)/2} \quad (8b)$$

$$\Delta\tau_{r,\theta} = (\sigma_1' - \sigma_2')[2(r_1^2 - r_2^2)/r^2 - 3(r_1^4 - r_2^4)/r^4](\sin 2\theta)/2 \quad (8c)$$

The radial relieved strain at any point $p(r, \theta)$ can be obtained by substituting the relieved stresses into Hooke's law:

$$\epsilon_{r,u} = \sigma_1'(A' + B'\cos 2\theta) + \sigma_2'(A' - B'\cos 2\theta) \quad (9)$$

where

$$\begin{aligned} A' &= [(1 + \nu)/(2E)][(r_1^2 - r_2^2)/r^2] \\ B' &= [(1 + \nu)/(2E)][\{4/(1 + \nu)\}[(r_1^2 - r_2^2)/r^2] - 3(r_1^4 - r_2^4)/r^4] \end{aligned}$$

The effect of the gauge area is also considered according to the foregoing procedures. The longitudinal relieved strain at any point $p(r, \phi)$ after VSR can be expressed as:

$$\begin{aligned} \epsilon_{u,u} = & \{(1 + \nu)[(r_1^2 - r_2^2)/(2r^2)](\sigma_1' + \sigma_2')\cos 2\phi \\ & + (1 - \nu)[(r_1^2 - r_2^2)/r^2](\sigma_1' - \sigma_2')\cos 2(\theta + \phi) \\ & + [(1 + \nu)/2][2(r_1^2 - r_2^2)/r^2 - 3(r_1^4 - r_2^4)/r^4] \\ & (\sigma_1' - \sigma_2')\cos 2(\theta + 2\phi)\}/E \end{aligned} \quad (10)$$

Accordingly, the average longitudinal relieved strain in the present condition can be acquired by the double integration:

$$\begin{aligned} \epsilon_{u,u} &= (1/2cw) \int_h^{h+c} \int_{-w}^w \epsilon_{u,u} du dv \\ &= A'(\sigma_1' + \sigma_2')/E + [B'(\sigma_1' - \sigma_2')\cos 2\theta]/E \end{aligned} \quad (11)$$

where

$$\begin{aligned} A' &= [(1 + \nu)(r_1^2 - r_2^2)/(2cw)]\{\tan^{-1}[(h+c)/w] - \tan^{-1}(h/w)\} \\ B' &= [1/(2cw)]\{2(1 - \nu)(r_1^2 - r_2^2)[\tan^{-1}((h+c)/w) - \tan^{-1}(h/w)] \\ &+ (1 + \nu)[2(r_1^2 - r_2^2)(-w(h+c)/((h+c)^2 + w^2) \\ &+ wh/(h^2 + w^2)) - (r_1^4 - r_2^4)(-w(h+c)/((h+c)^2 + w^2)^2 \\ &+ wh/(h^2 + w^2)]\} \end{aligned}$$

The three longitudinal relieved strains, as shown in Fig. 5, after VSR treatment can be obtained as the following expressions:

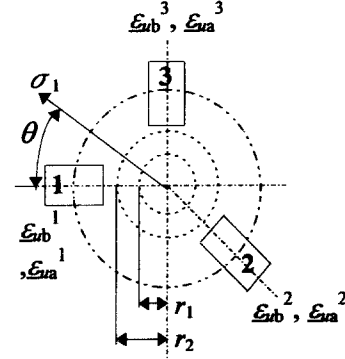


Fig. 5. The geometries and measured relieved strain of a commercially available strain gauge rosette.

$$\epsilon_{ua}^1 = A'(\sigma_1' + \sigma_2')/E + [B'(\sigma_1' - \sigma_2')\cos 2\theta]/E \quad (12a)$$

$$\epsilon_{ua}^2 = A'(\sigma_1' + \sigma_2')/E + [B'(\sigma_1' - \sigma_2')\cos 2(\theta + 225^\circ)]/E \quad (12b)$$

$$\epsilon_{ua}^3 = A'(\sigma_1' + \sigma_2')/E + [B'(\sigma_1' - \sigma_2')\cos 2(\theta + 90^\circ)]/E \quad (12c)$$

Therefore, the values and directions of the principal residual stresses after VSR treatment can be acquired by this modified hole-drilling method.

3. Preparation of the Experimental Specimens

In this study, we used 6061-T6 aluminium alloy with the following mechanical properties: Young's modulus = 69 000 MPa, yielding stress = 266 MPa, and Poisson's ratio = 0.33. Two pieces of thin butt-welded plates were prepared for the following experiments. These specimens were welded by the same TIG welding process, and held firmly with a fixture during welding.

The first specimen, shown in Fig. 6, was used to measure the originally locked-in residual stresses. The first set of principal residual stresses at the measured points (a_1) can be obtained by drilling a minor hole with a radius of r_1 through the centre of the cemented strain gauge rosette. Then the second set of the principal residual stresses at the same measured point can be obtained by enlarging the minor hole to a radius of r_2 . The above two sets of experimental results measured by the conventional hole-drilling method were used to check the deviation of the measured principal residual stresses between these two concentric drilled holes when the difference between the radii of the two drilled holes was quite small. The data of the other measured points (a_2 – a_5) can be acquired by the same processes.

The second specimen, shown in Fig. 7, was prepared to verify the accuracy of the modified hole-drilling method and to evaluate the effectiveness of the application of VSR. The original principal residual stresses before VSR were measured on the lefthand side (b_1 – b_5) of this specimen by drilling a minor hole with a radius of r_1 , and the results were compared with those derived from the first specimen. After VSR treatment, the principal residual stresses on the lefthand side were obtained by the modified hole-drilling method by enlarging the

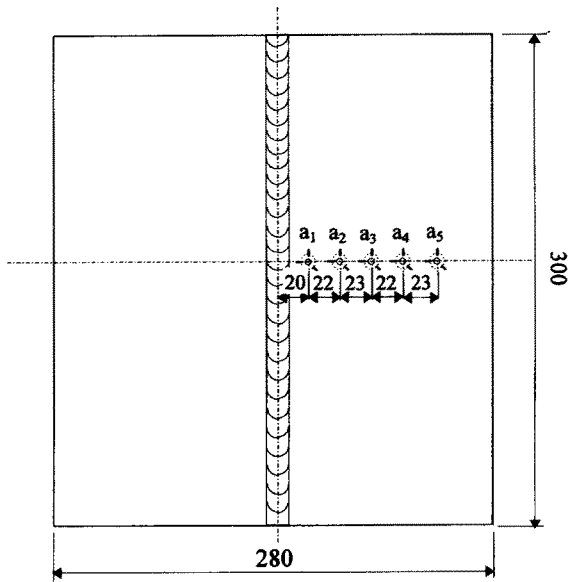


Fig. 6. Dimensions of the first thin butt-welded specimen and locations of the strain gauge rosettes (units in mm) for the measurement of the originally locked-in residual stresses (thickness = 2 mm).

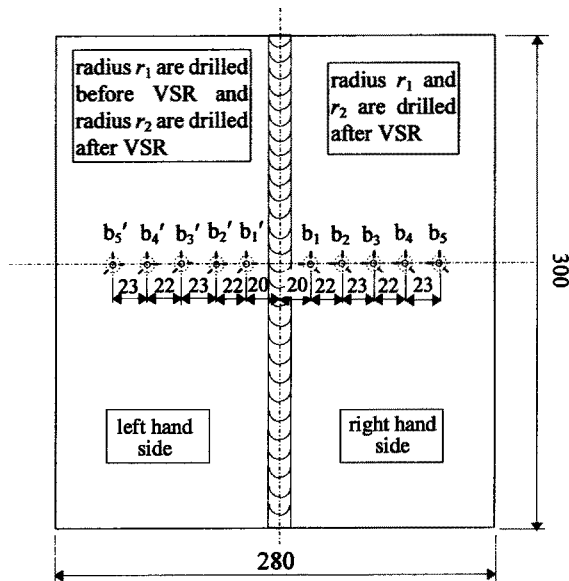


Fig. 7. Dimensions of the second thin butt-welded specimen and locations of the strain gauge rosettes (units in mm) for the measurement of the residual stresses before and after VSR treatment (thickness = 2 mm).

minor hole to a radius of r_2 . As a result, the effectiveness of VSR treatment can be established. Two sets of principal residual stresses after VSR on the righthand side (b_1 – b_5) of this specimen can be measured by the conventional hole-drilling method by drilling two concentric holes. The accuracy of the modified hole-drilling method can be verified by comparing the measured principal residual stresses with those acquired by the conventional hole-drilling method.

4. Experimental Work

The graphical representation of the experimental set-up of the VSR system is shown in Fig. 8. The commercially available vibratory stress relief apparatus used in this study consists of an a.c. electric motor with masses mounted eccentrically on its shaft to produce vibration. This apparatus also contains a power supply and control system to vary the motor speed from 0 to 180 Hz. A simple vibration table supported on four rubber pads was used in this investigation. The specimen was clamped at the central edge of the vibration table on which the unbalanced motor was also fastened at the corresponding central edge. An accelerometer was attached to the specimen near the welding region so as to detect the resonant frequencies. The first three resonant frequencies were observed to be 69, 129 and 150 Hz. Then, the system was vibrated for 20 min for each of these three resonant frequencies.

During the experiments, the RS-200 ultra-high-speed hole-drilling equipment was used to minimise the influence of the induced drilling stresses [24,25]. The schematic drawings of the locations of the strain gauges for measuring residual stresses are shown in Figs 6 and 7. To prevent an interactive effect between holes, the centre distance between two holes should be greater than three times the diameter of the drilled hole [26]. Therefore, the centre distances between the holes, as shown in Figs. 6 and 7, all met the requirements. According to the ASTM standards [21], the radius of the drilled hole should obey the following equation: $0.3 < [(r_1 \text{ or } r_2)/R] < 0.5$. Thus, the radii (0.8 and 1.2 mm) of the holes drilled in the experiments are all within the required ranges for $R = 2.565$ mm.

Commercially available three-element strain gauge rosettes with dimensions $c = 1.57$ mm, $h = 1.778$ mm, $w = 0.79$ mm, and $R = 2.565$ mm were cemented on the specified positions of the specimens. The values of **A** and **B** used in the conventional hole-drilling method versus R/a for various Poisson ratios are plotted in Fig. 9. In this study, the coefficients of the relieved strains after drilling a small hole with a radius of 0.8 mm are: **A** = -0.0639 and **B** = -0.1484 , and the coefficients of the relieved strains after enlarging the hole to a radius of 1.2 mm are: **A** = -0.1438 and **B** = -0.285 . The values of **A'** and **B'** used in the modified hole-drilling method versus R/a for various Poisson ratios are plotted in Fig. 10. In this study, the coefficients of the relieved strains after enlarging the hole to a radius of 1.2 mm are: **A'** = -0.08 and **B'** = -0.1367 .

Moreover, in order to preclude eccentricity occurring in the process of enlarging the drilled hole, a special tool with a guiding rod at its front end was designed and ground as shown in Fig. 11.

5. Presentation of the Results and Discussion

The first welding specimen as shown in Fig. 6 was used to measure the originally existing residual stresses remaining in the specified points (a_1 – a_5). The readings of the strain gauge

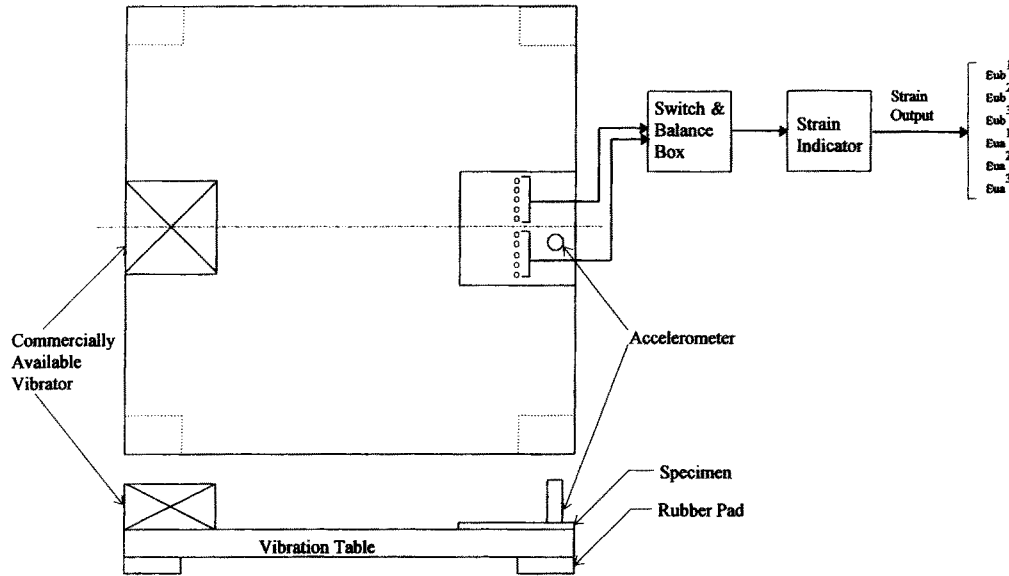


Fig. 8. Schematic representation of the set-up of the application of VSR.

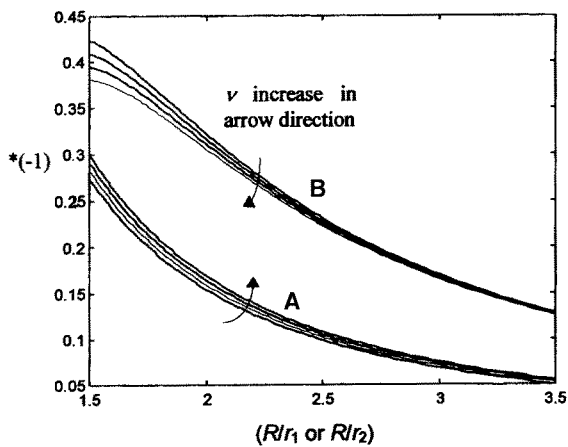


Fig. 9. Longitudinal relieved-strain coefficients A and B used in the conventional hole-drilling method for $c = 1.57$ mm, $h = 1.778$ mm, $w = 0.79$ mm, $R = 2.565$ mm, and various Poisson ratios ($\nu = 0.25, 0.29, 0.33, 0.37$).

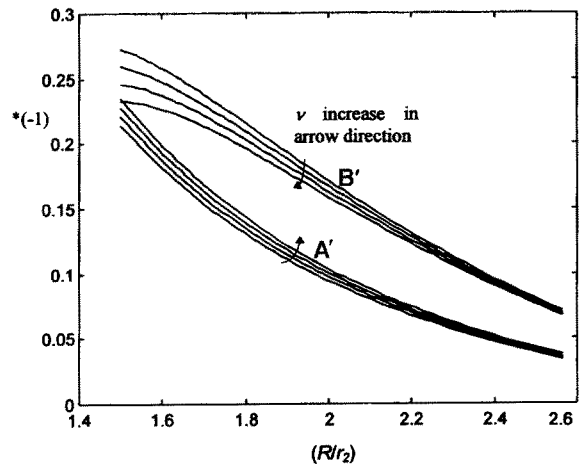


Fig. 10. Longitudinal relieved-strain coefficients A' and B' used in the proposed method for $c = 1.57$ mm, $h = 1.778$ mm, $w = 0.79$ mm, $R = 2.565$ mm, and various Poisson ratios ($\nu = 0.25, 0.29, 0.33, 0.37$).

rosettes from the strain indicator are shown in Table 1. By means of the conventional hole-drilling method, the measured principal residual stresses after drilling a minor hole with a radius of r_1 (0.8 mm) at each point and after enlarging the minor hole to a radius of r_2 (1.2 mm) are obtained as shown in Table 4. From the results, the deviations of the measured principal residual stresses between these two concentric drilled holes at all the measured points are all less than 4.2% owing to the limited difference in the radii of the concentric drilled holes in this investigation. Therefore, the principal residual stresses obtained were observed to be extremely close, as the radii of the two concentric drilled holes are 0.8 and 1.2 mm.

The second welding specimen, as shown in Fig. 7, was used to check the validity of the modified hole-drilling method compared to that of the conventional hole-drilling method and to determine the effectiveness of the application of the VSR

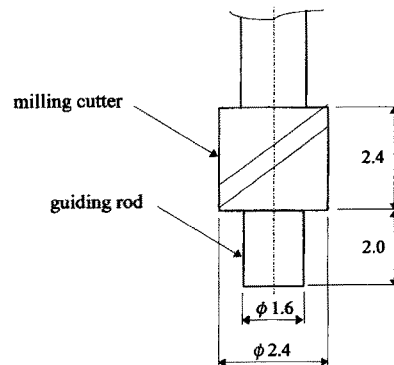


Fig. 11. Special tool ground to avoid eccentricity during the enlarging of the minor drilled hole (mm).

Table 1. Readings of the strain gauges from strain indicator for the first welding specimen.

Radius of the drilled hole (mm)	Readings ($\mu \epsilon$)	a_1	a_2	a_3	a_4	a_5
$r_1 = 0.8$	ϵ_{ub}^1	-410	-219	-130	-147	-115
$r_1 = 0.8$	ϵ_{ub}^2	-133	-70	39	69	23
$r_1 = 0.8$	ϵ_{ub}^3	-62	-15	121	185	112
$r_2 = 1.2$	ϵ_{ub}^1	-864	-459	-250	-275	-220
$r_2 = 1.2$	ϵ_{ub}^2	-338	-177	73	140	45
$r_2 = 1.2$	ϵ_{ub}^3	-173	-70	230	361	215

Table 2. Readings of the strain gauges from strain indicator for the second welding specimen (on the lefthand side), where radius = r_1 is measured before VSR and radius = r_2 is measured after VSR.

Radius of the drilled hole (mm)	Readings ($\mu \epsilon$)	b'_1	b'_2	b'_3	b'_4	b'_5
$r_1 = 0.8$	ϵ_{ub}^1	-404	-214	-131	-143	-115
$r_1 = 0.8$	ϵ_{ub}^2	-136	-65	37	65	23
$r_1 = 0.8$	ϵ_{ub}^3	-55	-15	118	179	109
$r_2 = 1.2$	ϵ_{ua}^1	-328	-196	-112	-116	-98
$r_2 = 1.2$	ϵ_{ua}^2	-139	-80	27	52	19
$r_2 = 1.2$	ϵ_{ua}^3	-85	-43	97	147	89

Table 3. Readings of the strain gauges from strain indicator for the second welding specimen (on the righthand side), where radius = r_1 and radius = r_2 are all measured after VSR.

Radius of the drilled hole (mm)	Readings ($\mu \epsilon$)	b_1	b_2	b_3	b_4	b_5
$r_1 = 0.8$	ϵ_{ua}^1	-318	-188	-117	-131	-102
$r_1 = 0.8$	ϵ_{ua}^2	-92	-52	32	54	21
$r_1 = 0.8$	ϵ_{ua}^3	-28	-7	108	160	96
$r_2 = 1.2$	ϵ_{ua}^1	-639	-384	-228	-247	-200
$r_2 = 1.2$	ϵ_{ua}^2	-236	-136	62	107	41
$r_2 = 1.2$	ϵ_{ua}^3	-130	-53	204	307	185

Table 4. Measured original principal residual stresses and the percentage of the relative errors between the two concentric drilled holes ($r_1 = 0.8$ mm and $r_2 = 1.2$ mm) for the first welding specimen.

Position	Strain gauge rosette positions and percentage of the relative errors														
	a_1			a_2			a_3			a_4			a_5		
	r_1	r_2	error (%)	r_1	r_2	error (%)	r_1	r_2	error (%)	r_1	r_2	error (%)	r_1	r_2	error (%)
σ_1	174.8	171.6	1.8	89.5	89.4	0.1	33.2	33.2	0	30.1	30.0	0.3	27.7	27.7	0
σ_2	80.6	77.2	4.2	37.2	37.7	1.3	-28.6	-28.4	0.7	-50.5	-50.6	0.2	-26.3	-26.3	0

process. The readings ($\epsilon_{ub}^1 - \epsilon_{ub}^3$) of the strain gauge rosettes on the lefthand side (b'_1 - b'_5) after drilling a minor hole with a radius of r_1 (0.8 mm) at each point are shown in Table 2. The original principal residual stresses in this specimen can be calculated and are given in Table 5.

After VSR treatment at the first three resonant frequencies, the drilled holes on the lefthand side were enlarged to a radius of r_2 , the readings ($\epsilon_{ua}^1 - \epsilon_{ua}^3$) of the strain gauge rosettes are presented in Table 2, and the principal residual stresses after VSR are measured by the modified hole-drilling method, as shown in Table 5. The readings of the strain gauge rosettes on the righthand side (b_1 - b_5) after drilling a minor hole with a radius of r_1 and enlarging it to a radius of r_2 at each point are displayed in Table 3, and the principal residual stresses after VSR are measured by the conventional hole-drilling method, as shown in Table 6. The deviations of the measured principal residual stresses between the two concentric drilled holes at the measured points on the righthand side are all within 3.3%. Accordingly, the measured principal residual stresses for the two concentric drilled holes on the righthand side after VSR with radii of 0.8 and 1.2 mm at each point can be thought of as being identical to the results derived from the first specimen.

Since the effect of the VSR process on the second specimen is symmetric, the distribution of the residual stresses on the two sides after VSR should be identical. The percentages of the relative error of the measured principal residual stresses (radius = r_2) after VSR at each point between the modified and conventional hole-drilling method are all below 2.9% as shown in Table 7. Thus, the modified hole-drilling method proves to be accurate after being compared with the conventional hole-drilling method. Furthermore, the percentage of the effectiveness after the VSR treatment in the measured points

can be obtained by $[(\sigma_1)_{r_1} - (\sigma_1)_{r_2}] / (\sigma_1)_{r_1}$ and $[(\sigma_2)_{r_1} - (\sigma_2)_{r_2}] / (\sigma_2)_{r_1}$, and the results are expressed in Table 5. The maximum percentage effectiveness in this study is observed at measured point b'_1 ; i.e. 27% for the maximum principal residual stress (σ_1) and 31% for the minimum principal residual stress

Table 5. Measured principal residual stresses and percentage of the effectiveness after VSR treatment for the second welding specimen (on the lefthand side), where the values (radius = r_1) are measured before VSR, and the values (radius = r_2) are measured by means of the modified hole-drilling method after VSR.

Position	Strain gauge rosette positions and percentage of the effectiveness of the treatment of VSR														
	b'_1			b'_2			b'_3			b'_4			b'_5		
Measured values (MPa)	r_1	r_2	(%)	r_1	r_2	(%)	r_1	r_2	(%)	r_1	r_2	(%)	r_1	r_2	(%)
$(\sigma_1 \text{ and } \sigma'_1)$	170.3	124.3	27	87.6	73.5	16.1	34.1	31.2	8.5	29.5	27.8	5.8	28.6	26.3	8.0
$(\sigma_2 \text{ and } \sigma'_2)$	78.1	53.9	31	35.9	29.8	17.0	-27.3	-24.5	10.3	-48.6	-41.3	15.0	-24.9	-22.5	9.6

Table 6. Measured principal residual stresses and their percentage of the relative errors between the two concentric drilled holes ($r_1 = 0.8$ mm and $r_2 = 1.2$ mm) using the conventional hole-drilling method for the second welding specimen (on the righthand side) after VSR.

Position	Strain gauge rosette positions and percentage of the relative errors														
	b_1			b_2			b_3			b_4			b_5		
Measured values (MPa)	r_1	r_2	error (%)	r_1	r_2	error (%)	r_1	r_2	error (%)	r_1	r_2	error (%)	r_1	r_2	error (%)
σ'_1	132.2	128.0	3.2	76.4	74.9	2.0	29.9	30.5	2.0	27.2	27.6	1.5	25.4	25.8	1.6
σ'_2	54.8	56.6	3.3	29.1	30.0	3.1	-25.2	-24.8	1.6	-42.8	-42.0	1.9	-22.1	-22.3	0.9

Table 7. Measured principal residual stresses and percentage of the relative error after VSR treatment for the second welding specimen. The values are measured by the modified hole-drilling method on the lefthand side (b'_1 - b'_5), and the values are measured by the conventional hole-drilling method on the righthand side (b_1 - b_5).

Measured values (MPa)	Strain gauge rosette positions and percentage of the relative error with a radius of r_2														
	b_1	b'_1	error (%)	b_2	b'_2	error (%)	b_3	b'_3	error (%)	b_4	b'_4	error (%)	b_5	b'_5	error (%)
σ'_1	128.0	124.3	2.9	74.9	73.5	1.9	30.5	31.2	2.3	27.6	27.8	0.7	25.8	26.3	1.9
σ'_2	56.6	53.9	0.7	30.0	29.8	0.7	-24.8	-24.5	1.2	-42.0	-41.3	1.7	-22.3	-22.5	0.9

(σ_2). The distributions of the measured principal residual stresses in the second welding specimen before and after the treatment of the VSR process are plotted in Fig. 12.

6. Conclusions

The investigation described in this paper leads to the following conclusions:

1. A modified hole-drilling method for the determination of the principal residual stresses at the same point in thin plates before and after VSR treatment is developed, and the validity of this method is confirmed by comparison with the conventional hole-drilling method.
2. Since the deviations of the measured principal residual stresses between the two concentric drilled holes at any measured point both before and after VSR are all within 4.2% owing to the limited difference of the radii of the

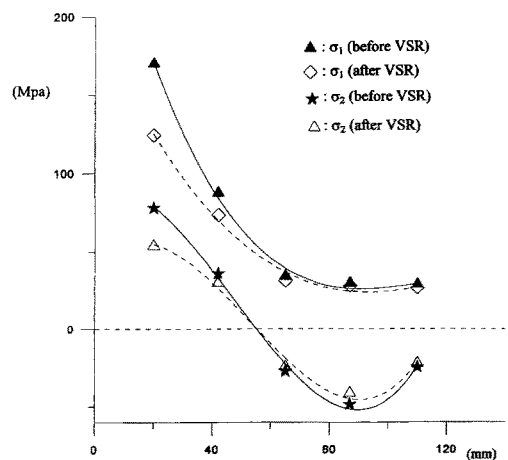


Fig. 12. Distribution of the principal residual stresses in the second welding specimen before and after VSR treatment.

concentric drilled holes, the obtained principal residual stresses at any measured point can be considered to be identical for drilled holes of 0.8 and 1.2 mm radius.

3. The effectiveness of VSR treatment can be measured by comparing the measured residual stresses at the same measured points before and after the VSR process.
4. The eccentricity between the minor and enlarged drilled holes can be effectively prevented with a specially designed and ground tool.
5. The application of VSR at the first three resonant frequencies in this study effectively reduces the residual stresses locked in the welding specimen.

References

1. D. A. Hills, R. B. Waterhouse and B. Noble, "An analysis of shot peening", *Journal of Strain Analysis*, 18(2), pp. 95–100, 1983.
2. V. S. Biront, V. A. Sushchikh, E. V. Yuzhakova, A. S. Fofanova and T. V. Baidina, "Relaxation of residual stresses in ultrasonic treatment", *Metal Science and Heat Treatment*, 31(5), pp. 467–470, November 1989.
3. A. G. Olabi and M. S. J. Hashmi, "Stress relief procedures for low carbon steel (1020) welded components", *Journal of Materials Processing Technology*, 56, pp. 552–562, 1996.
4. C. C. Weng and J. J. Chen, "Study on residual stress relief of welded structural steel joints", *Journal of Materials in Civil Engineering*, 5(2), pp. 265–279, May 1993.
5. S. R. Rich, "Tried vibratory stress relief", *American Mechanist*, pp. 110–111, April 1968.
6. S. Weiss, G. S. Baker and R. D. Das Gupta, "Vibrational residual stress relief in a plain carbon steel weldment", *Welding Research Supplement*, pp. 47-s–51-s, February 1976.
7. G. August and J. Hebel, "Subresonant vibrations relieve residual stress", *Metal Progress*, pp. 51–55, November 1985.
8. G. P. Wonzney and G. R. Crawmer, "An investigation of vibrational stress relief in steel", *Welding Research Supplement*, pp. 411-s–419-s, September 1968.
9. R. Dawson and D. G. Moffat, "Vibratory stress relief: a fundamental study of its effectiveness", *Transactions ASME, Journal of Engineering Materials and Technology*, 102, pp. 169–176, April 1980.
10. B. B. Klauba and C. M. Adamas, "A progress on the use and understanding of vibratory stress relief", *Proceedings of the Winter Annual Meeting of the ASME, AMD 52*, pp. 47–57, 1982.
11. C. Balasingh, M. R. Seshadri, M. N. Srinivasan and S. Ramaseshan, "Vibrational stress-relief of cast iron castings", *Indian Foundry Journal*, pp. 129–136, November 1983.
12. E. P. Olenin, A. S. Averin, E. V. Dobrotina and O. K. Alekseev, "Reducing the residual stresses in welded components by vibrational method", *Welding Production*, pp. 19–21, May 1983.
13. M. Jesensky, "Vibratory lowering of residual stresses in weldments", *Proceeding of IIW Conference, Sofia*, pp. 153–160, July 1987.
14. R. A. Claxton and A. Lupton, "Vibratory stress relieving of welded fabrications", *Welding and Metal Fabrications*, pp. 541–544, December 1991.
15. C. A. Walker, A. J. Waddell and D. J. Johnston, "Vibratory stress relief – an investigation of the underlying processes", Part E: *Journal of Process Mechanical Engineering*, 209, pp. 51–58, 1995.
16. C. Bouhelier, P. Barbarin, J. P. Deville and B. Miede, "Vibratory stress relief of welded parts", *Mechanical Relaxation of Residual Stress, ASTM STP 993*, pp. 58–71, 1988.
17. R. D. Ohol, B. V. Nagendra Kumar and R. A. Noras, "Measurement of vibration-induced stress relief in the heavy fabrication industry", *Mechanical Relaxation of Residual Stress, ASTM STP 993*, pp. 45–57, 1988.
18. G. S. Schajer, "Application of finite element calculations to residual stress measurements", *Transactions ASME, Journal of Engineering Materials and Technology*, 103, pp. 157–163, April 1981.
19. N. J. Rendler and I. Vigness, "Hole-drilling strain-gage method of measuring residual stresses", *Experimental Mechanics*, pp. 577–586, December 1966.
20. Bulletin TN-503-4, "Measurement of residual stresses by the hole-drilling strain gage method", pp. 1–19, 1993.
21. ASTM-E837-92, "Standard test method for determining residual stress by the hole-drilling strain-gage method", pp. 747–753, 1992.
22. M. Kabiri, "Nonuniform residual-stress measurement by hole-drilling method", *Experimental Mechanics*, pp. 328–336, December 1984.
23. J. Y. Wang, "Refined analysis of the relieved strain coefficients for the off-center hole-drilling case", *Experimental Mechanics*, pp. 367–371, December 1990.
24. M. T. Flaman, "Brief investigation of induced drilling stresses in the center-hole method of residual-stress measurement", *Experimental Mechanics*, pp. 26–30, January 1982.
25. M. T. Flaman and J. A. Herring, "Comparison of four hole-producing techniques for the center-hole residual-stress measurement method", *Experimental Technique*, pp. 30–32, 1985.
26. A. M. Nawwar and J. Shewchuk, "On the measurement of residual stress gradients in aluminum-alloy", *Experimental Mechanics*, pp. 269–276, July 1978.

Nomenclature

A, B	coefficient of the relieved strain
A, B	coefficient of the relieved strain including the gauge area effect due to drilling a hole with a radius of r_1 or r_2 for the conventional hole-drilling method
A', B'	coefficient of the relieved strain after VSR
A', B'	coefficient of the relieved strain including the gauge area effect due to enlarging the minor hole with a radius of r_2 for the modified hole-drilling method
E	Young's modulus
R	radius of the gauge circle
r_1	radius of the minor drilled hole
r_2	radius of the enlarged drilled hole
c	gauge length
h	distance from the front point of the gauge to the centre of the gauge circle
r	distance from the centre of the gauge circle to any specified point of the strain gauge
u	longitudinal direction of a strain gauge
v	transverse direction of a strain gauge
w	half of the gauge width
θ	angle measured from the direction of σ_1
ϕ	angle measured from the longitudinal direction
ν	Poisson's ratio
ϵ_{rb}	radial relieved strain before VSR
ϵ_{ra}	radial relieved strain after VSR
$\epsilon_{ubs}^1, \epsilon_{ub}^1, \epsilon_{ub}^2, \epsilon_{ub}^3$	average longitudinal relieved strain before VSR
$\epsilon_{uas}^1, \epsilon_{ua}^1, \epsilon_{ua}^2, \epsilon_{ua}^3$	average longitudinal relieved strain after VSR
σ_1	maximum principal residual stress (MPa) before VSR
σ_2	minimum principal residual stress (MPa) before VSR
σ'_1	maximum principal residual stress (MPa) after VSR
σ'_2	minimum principal residual stress (MPa) after VSR
$\sigma'_{r, \sigma'_\theta, \tau'_{\theta r}}$	stress in the vicinity of the hole with a radius of r_1 after VSR
$\sigma''_r, \sigma''_\theta, \tau''_{\theta r}$	stress in the vicinity of the hole with a radius of r_2 after VSR
$\Delta\sigma_r, \Delta\sigma_\theta, \Delta\tau_{\theta r}$	relieved stress after enlarging the minor hole with a radius of r_2 after VSR